Journal of Hazardous Materials 201–202 (2012) 162–169

Contents lists available at SciVerse ScienceDirect

Journal of Hazardous Materials

journal homepage: www.elsevier.com/locate/jhazmat

Glow discharge plasma in water: A green approach to enhancing ability of chitosan for dye removal

Yuezhong Wen[a,c,*], Chensi Shen[a], Yanyan Ni[b], Shaoping Tong[b], Feng Yu[c]

[a] Institute of Environmental Science, Zhejiang University, Hangzhou 310058, China
[b] College of Chemical Engineering and Materials Science, Zhejiang University of Technology, Hangzhou 310032, China
[c] Zhejiang Chemical Industry Research Institute, Hangzhou 310023, China

ARTICLE INFO

Article history:
Received 18 May 2011
Received in revised form 31 October 2011
Accepted 17 November 2011
Available online 25 November 2011

Keywords:
Glow discharge plasma
Chitosan
Surface modification
Pretreatment
Dye
Removal

ABSTRACT

There is a need to explore effective and green approaches to enhancing the ability to use chitosan for contaminant removal for practical implementation of this technology. In the present study, glow discharge plasma (GDP), which has thus far been studied for degradation of contaminants, was used for the first time to pre-treat chitosan for dye removal in aqueous solution. The results show that the GDP treatment changed the morphology and crystallinity of chitosan particles, and the number of $-CH_2$ and $-CH_3$ groups in the chitosan samples increased. Various pretreatment parameters, including discharge current and time, played significant roles in the chitosan modification. It is observed that dye uptake in GDP-modified chitosan was faster than adsorption in untreated chitosan. The maximum adsorption by chitosan followed the order of untreated chitosan < modified chitosan (GDP current: 50 mA) < modified chitosan (GDP current: 120 mA), implying that the chitosan modified by GDP had a higher maximum adsorption capacity in comparison with the untreated chitosan. A possible mechanism is proposed. These results show that GDP may be an attractive pretreatment technology for environmental adsorption materials.

1. Introduction

Chitosan, the deacetylated product of chitin, is a renewable biopolymer. Due to its biocompatibility, biodegradability, lack of toxicity, low cost and abundance in nature, chitosan has attracted considerable attention for its environmental applications, especially for the removal of dye pollutants, which are a serious source of environmental contamination in many countries [1,2]. Because chitosan contains a large number of active hydroxyl (–OH) and amine ($-NH_2$) groups, it exhibits good adsorption capacity for anionic dyes and heavy metal ions. Nevertheless, for the practical application of chitosan, there is a need to develop methods for enhancing the adsorption capacity of chitosan.

Recently, much attention has been paid to developing suitable methods for chitosan modification, including monocarboxymethylation, cross linking with epichlorohydrin, cross linking with polyvinyl alcohol blend beads and incorporation in magnetic resins [3–6]. However, such modifications require inconvenient procedures and large quantities of organic solvents. Therefore, there still remains a need to explore new and green approaches to enhancing the ability of chitosan to remove contaminants from water.

Non-thermal plasmas, such as dielectric barrier discharge, corona discharge, and glow discharge, are a great alternative technology for degradation of aqueous organic pollutants [7–10]. Among these plasma technologies, glow discharge plasma (GDP) is now considered as a promising advanced oxidation technology due to its stable operation, low discharge and much higher yields of oxidizing species, such as •OH and H_2O_2, produced in the liquid-phase when compared with what is expected on the basis of Faraday's law [11,12]. In addition, GDP can be run in water with higher conductivity compared with pulsed corona discharge plasma [13–15]. Nevertheless, most environmental research on glow discharge plasma has thus far been focused on investigating the degradation of contaminants. Today, gas plasma-based strategies for the surface modification of biodegradable polymers and biomaterials have demonstrated great potential [16,17]. In this regard, gases are applied during the plasma treatment process. As a result, chemical functionalities are introduced onto the surfaces of the materials. The introduced functionalities can be subsequently used to bind polymers or other molecules to the surface in order to achieve desired surface properties [18]. However, application of glow discharge plasma in water to modify bio-macromolecules for the adsorption of hazardous compounds has not been reported.

Our recent work showed that chitosan could be efficiently pretreated with H_2O_2 to induce modifications that allow improved removal of C. I. Acid Red 73 from weak acid solutions [19]. The

* Corresponding author at: Institute of Environmental Science, Zhejiang University, Hangzhou 310058, China. Tel.: +86 571 8898 2344; fax: +86 571 8898 2344.
E-mail address: wenyuezhong@zju.edu.cn (Y. Wen).

0304-3894/$ – see front matter © 2011 Elsevier B.V. All rights reserved.
doi:10.1016/j.jhazmat.2011.11.057

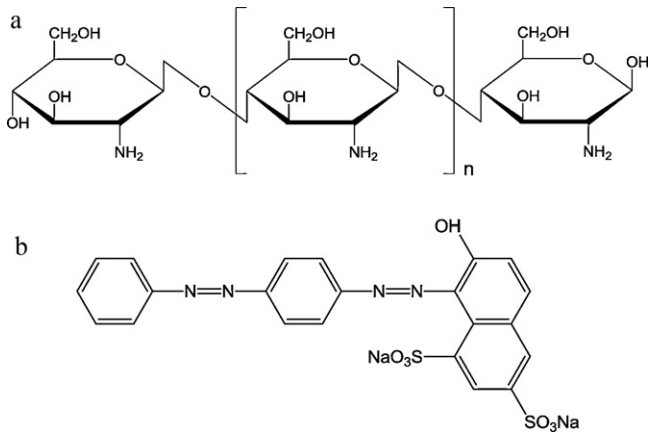

Fig. 1. The chemical structures of (a) chitosan and (b) C. I. Acid Red 73.

pretreated chitosan appeared to have a more ordered structure and a higher hydrophilic character than the untreated chitosan, but no significant changes in functional groups on the chitosan surface were detected. Capitalizing on the fact that glow discharge plasma in water can also generate active oxygen species, we hypothesized that it might be possible to explore a plasma approach to enhance the adsorption capacity of chitosan. Herein, the pretreatment of chitosan by glow discharge plasma in water is reported, and the effects of various pretreatment parameters on the modification of chitosan were investigated.

2. Materials and methods

2.1. Chemicals

Chitosan was purchased from Zhejiang Golden-shell Biochemical Co., Ltd., Zhejiang, China (deacetylation degree = 91.04%, Fig. 1a). C. I. Acid Red 73 (AR 73, chemical structure is shown in Fig. 1b) and other dyes are all commercially available. Doubly distilled water was used throughout this study. Other chemicals were of laboratory reagent grade and used without further purification.

2.2. Modification of chitosan via glow discharge plasma

The GDP reactor contained a cylindrical vessel with an inner diameter of 40 mm. The DC high-voltage power unit (variable voltage of 0–600 V and current of 0–600 mA) was supplied by Beijing Da Hua Radio Factory. The anode, from which the discharge was emitted, was a pointed platinum wire (Id 0.6 mm) sealed into a glass tube. The cathode was a stainless steel plate placed in another glass tube and separated from the anodic compartment by a glass frit of medium porosity. The solution was maintained at 298 ± 2 K by circulation through a water-cooled jacket.

During the modification procedure, chitosan powder (1.0 g) was suspended in a 150 mL sodium sulfate solution (Na_2SO_4 concentration: 2 g/L; conductivity: 2320 μS/cm). A DC high voltage of 530 V was applied across the electrodes through a DC power source to start the modification. The modified chitosan powder was collected by centrifugation at 5000 rpm, washed with a large amount of water to remove the remaining byproducts produced in the GDP reaction and then dried in oven at 80 °C.

The H_2O_2 formed during the glow discharge process was determined using a UV-visible spectrometer (UV-2401PC, Shimadzu, Japan) with a colorimetric method [20].

2.3. Characteristics of untreated chitosan and modified chitosan

Surface morphology was studied with an electron microscope. The scanning electron micrographs (SEMs) of chitosan were obtained with a field emission scanning electron microscope (FEI, SIRON) at a voltage of 25.0 kV. The sample surfaces were gold-coated before analysis. X-ray diffraction (XRD) patterns of the chitosan sample were measured using a Panalytical XPert Pro MPD diffractometer with a Cu Kα X-ray source ($\lambda = 1.54$ Å). The scanning diffraction angle range was set at 5–60° and the scan rate was 2° (2θ) per minute at 40 kV and 36 mA. The degree of crystallinity was calculated using the Material Data software Jade 5.0 to analyze the XRD data. Fourier transform infrared spectroscopy (FTIR) of chitosan samples was recorded on a Shimadzu 8900 FTIR spectrometer (Tokyo, Japan) using KBr power containing ca. 1% (w/w) of sample. X-ray photoelectron spectroscopy (XPS) was performed on an electron spectrometer from Thermo ESCALAB 250 (MA, US);

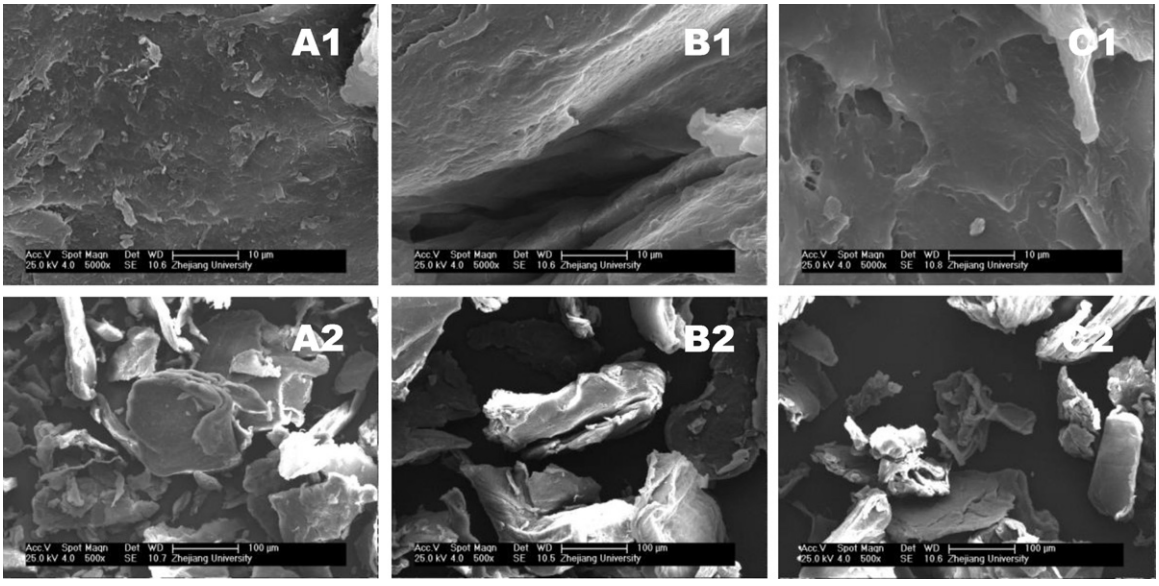

Fig. 2. Scanning electron micrographs (SEMs) of the untreated chitosan and GDP-modified chitosan at low and high magnification: (A1 and A2) untreated chitosan; (B1 and B2), GDP-modified chitosan (GDP current: 80 mA; reaction time: 30 min); (C1 and C2), GDP-modified chitosan (GDP current: 80 mA; reaction time: 60 min).

the samples were excited with X-rays over a specific 400-μm area using monochromatic Al Kα radiation (1486.6 eV) at 150 W. Chitosan (neutral form, as received) and modified chitosan samples were vacuum-dried at room temperature for 72 h before analysis. All binding energies were referenced to the neutral carbon peak at 284.8 eV, and surface elemental stoichiometries were determined from sensitivity-factor corrected peak ratios. Zeta potential measurements were determined at room temperature with the chitosan samples dispersed in deionized water by sonication. In these measurements, the pH of this dispersion was maintained at 6.0 ± 0.05 using 0.1 mol/L HCl for adjustment. The zeta potential, ζ, of untreated and modified chitosan was measured using a Zeta-Meter System 3.0 (Zeta-Meter Inc., USA).

2.4. Removal of dyes

All the dye adsorption experiments were performed in 50 mL flasks, which were sealed and agitated at 100 rpm in a thermostatic shaker maintained at 25 °C. The typical reaction mixture contained 10 mL of dye at 50 mg/L and 0.02 g of chitosan. The initial pH value of the dye solutions was adjusted to 6 by addition of 0.01 mol/L HCl. Dye concentrations were analyzed using a Shimadzu UV-2401PC UV-vis spectrometer (Tokyo, Japan) at its absorbance maximum.

The adsorption isotherms for the dye by chitosan in water were carried out using the batch slurry method. The slurry, containing 0.02 g of chitosan and 10 mL of AR 73 solution at various concentrations was agitated at 100 rpm in a thermostatic shaker until equilibrium was reached at a temperature of 25 °C. The amount of adsorbed AR 73, q_e, was calculated using Eq. (1):

$$q_e = \frac{(C_0 - C_e)V}{M} \quad (1)$$

where q_e is the dye capacity of the sorbent at equilibrium (mg/g), C_0 is the initial dye concentration in the liquid phase (mg/L), C_e is the liquid-phase dye concentration at equilibrium (mg/L), V is the volume of solution (L), and M is the mass of sorbent used (g).

3. Results and discussion

3.1. Plasma treatment of chitosan: morphology, structure and characterization analysis

Plasma is referred to as the fourth state of matter, which can be defined as a quasi-neutral particle system in the form of fluid-like mixtures of free electrons, ions and radicals, generally also containing neutral particles. In our experiments, plasma is generated by passing water through electrical fields during glow discharge. These plasmas show strong deviations from kinetic equilibrium and have electron temperatures that are much higher than the temperature of the ions and neutral species because electric energy is used to generate energetic electrons and other highly reactive plasma species, but not heat the background water. It is clear that plasma is a very reactive environment in which several different interactions between it and a surface are possible. Therefore, the morphology, structure and characterization of chitosan were analyzed after plasma treatment.

The morphology of the untreated and GDP-modified chitosan samples was examined by SEM (Fig. 2). Based on images A2, B2 and C2, both the untreated and modified chitosan samples were irregularly shaped and had a diameter between 100 and 200 μm. Changes in the external morphology were evaluated by comparing images in Fig. 2A1, B1 and C1. After the GDP modification at a current of 30 mA and 60 mA, the surface of modified chitosan was much smoother and most of the crude aspects of the untreated chitosan were removed. In addition, enhancement of the plasma current tends to improve this smoothing effect.

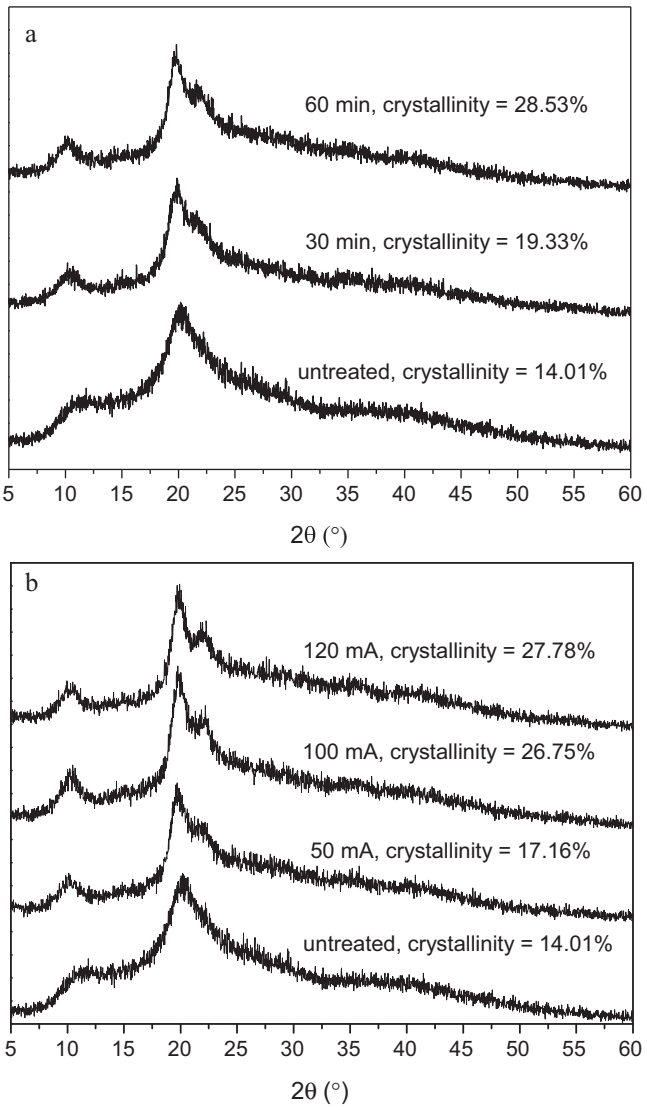

Fig. 3. X-ray diffraction patterns of chitosan modified at different (a) pretreatment times (GDP current: 80 mA) and (b) GDP currents (pretreatment time: 60 min).

To observe the structure of plasma-treated chitosan, X-ray diffraction patterns of untreated chitosan and chitosan that had been modified with GDP at different currents and reaction times (Fig. 3) were compared. With elevated GDP current (Fig. 3a) or increased reaction time (Fig. 3b), an increase in the intensity and sharpness of the characteristic peaks at $2\theta = 19.84^\circ$ and $2\theta = 10.38^\circ$ was observed, which accompanied an increase in the degree of crystallinity of the chitosan products. When the GDP modification time and current were increased to 60 min and 120 mA, the degree of crystallinity of the chitosan reached 28.53% and 27.78%, respectively, representing a 14.52% and 13.77% increase compared with untreated chitosan (crystallinity degree, 14.01%), which indicates the chitosan surface assumed a more ordered structure.

In addition, Fourier transform infrared (FTIR) spectroscopy was used to investigate the chemical nature of the chitosan samples. Fig. 4 presents the data of untreated chitosan and GDP-modified chitosan. The peaks at 3420 cm^{-1} (N–H), 1650 cm^{-1} (amide I band), 1590 cm^{-1} ($-NH_2$), 1259 cm^{-1} (twisting vibration of O–H), 1080 cm^{-1} (stretching vibration of the C–O–C in glucose), 1155 cm^{-1} and 897 cm^{-1} (characteristic peaks of $\beta(1 \rightarrow 4)$ glucoside) were similar to previously reported spectra of chitosan. However, peaks around 1380 cm^{-1} and 1430 cm^{-1}, which

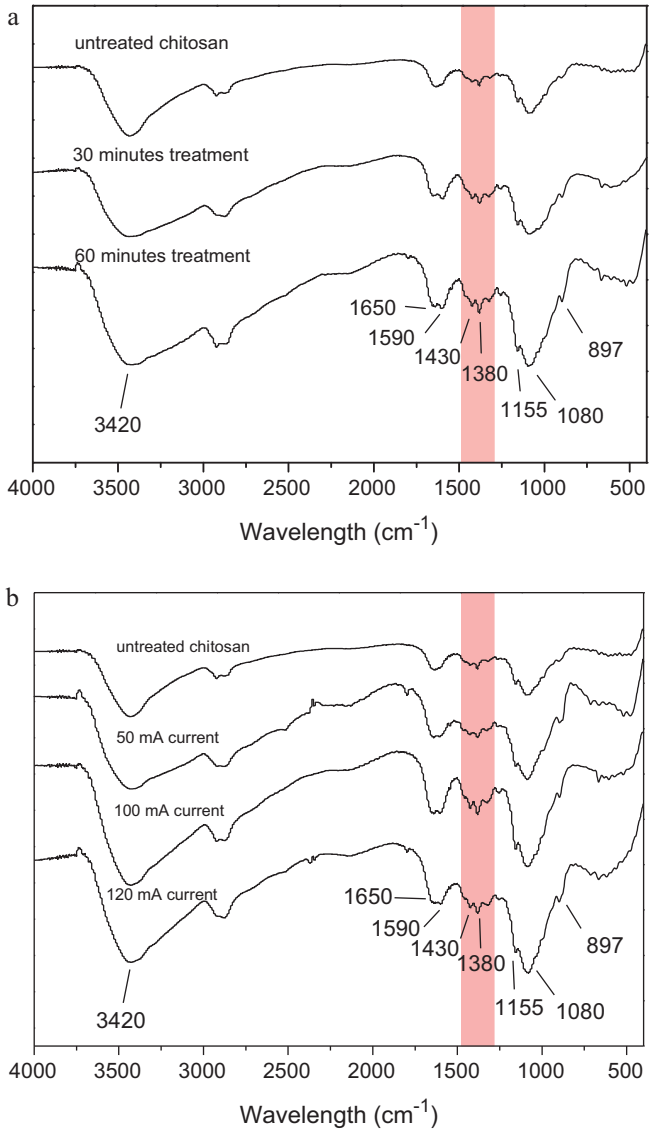

Fig. 4. FTIR spectra of chitosan modified at different (a) pretreatment time (GDP current: 80 mA) and (b) GDP currents (pretreatment time: 60 min).

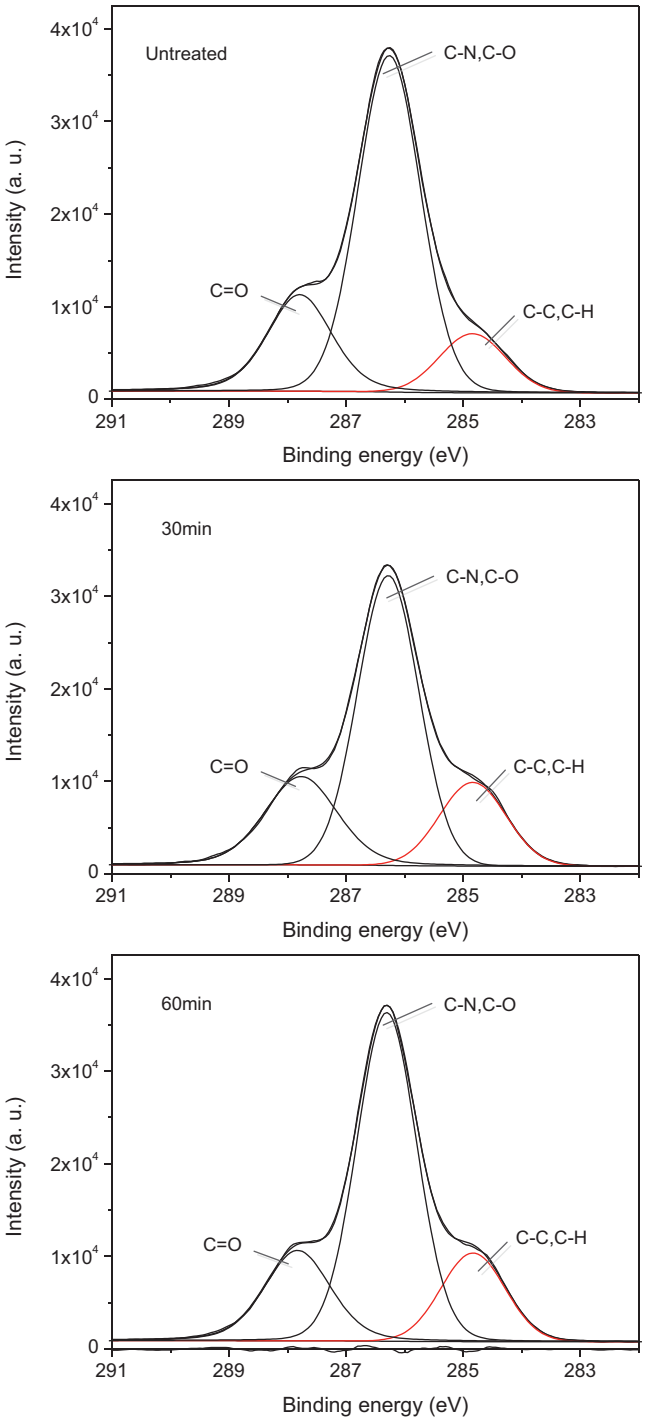

Fig. 5. XPS spectra of C 1s. (a) Untreated chitosan; (b) GDP-modified chitosan (GDP current: 80 mA; reaction time: 30 min); (c) GDP-modified chitosan (GDP current: 80 mA; reaction time: 60 min).

are related to $-CH_2$ and $-CH_3$ groups, appeared to be sharper after the GDP modification, suggesting the presence of a greater number of $-CH_2$ and $-CH_3$ groups in the modified chitosan.

Further, modification of the surface functional groups of chitosan after GDP treatment was investigated by XPS analysis. The elemental surface composition and the relative amounts of the different functional groups in untreated and modified chitosan were calculated and are summarized in Table 1. Except for the C 1s valence state, chitosan samples with or without modification have no prominent differences in the calculated relative amounts of other functional groups. Thus, the chemical changes on the surface were analyzed in more detail by recording the high-resolution carbon C 1s spectra of both untreated and GDP-modified chitosan samples. The C 1s spectra of the different samples are shown in Fig. 5. The C 1s spectrum of chitosan could be resolved into three sub-peaks at binding energies of 284.8 eV, 286.3 eV and 287.8 eV, which are characteristic of C–C or C–H, C–N or C–O and C=O, respectively. These data show a clear difference between the C 1s spectrum of the untreated chitosan and the spectra of GDP-modified chitosan. After GDP modification for 30 min and 60 min, the peak assigned to C–C or C–H in the C 1s spectrum of chitosan was enhanced, corresponding to a relative increase in this peak from 6.49% to 9.87% and 10.30%, respectively. This data is in agreement with the results of FTIR analysis; the enhanced C–C or C–H bonding could be attributed to an increase in the number of $-CH_2$ and $-CH_3$ groups in the chitosan samples after GDP modification.

According to the above results, the GDP treatment changed the morphology and crystallinity of the chitosan particles, while the number of $-CH_2$ and $-CH_3$ groups in the chitosan samples increased. This phenomenon could be explained by the peeling-off model of chitosan [21,22]. As has been reported in the literature,

Table 1
Binding energies and relative amounts of chemical groups on the chitosan surface.

	Proposed chemical groups	Binding energy (eV)	Relative amounts (at.%)
C 1s valence state			
(a) Untreated chitosan	C–C or C–H	284.8	6.49
	C–N or C–O	286.3	35.70
	C═O	287.8	11.66
(b) Modified chitosan (30 min)	C–C or C–H	284.8	9.87
	C–N or C–O	286.2	31.37
	C═O	287.8	12.44
(c) Pretreated chitosan (60 min)	C–C or C–H	284.8	10.30
	C–N or C–O	286.2	31.99
	C═O	287.8	12.05
N 1s valence state			
(a) Untreated chitosan	$-NH_2$	399.2	6.67
	$-NH_3^+$	400.2	1.03
	–NH–CO	401.7	0.47
(b) Pretreated chitosan (30 min)	$-NH_2$	399.2	5.94
	$-NH_3^+$	400.2	1.19
	–NH–CO	401.7	0.52
(c) Pretreated chitosan (60 min)	$-NH_2$	399.2	6.07
	$-NH_3^+$	400.2	1.02
	–NH–CO	401.7	0.65
O 1s valence state			
(a) Untreated chitosan	C–O–H or C–O–C	532.7	37.1
(b) Pretreated chitosan (30 min)	C–O–H or C–O–C	532.7	38.2
(c) Pretreated chitosan (60 min)	C–O–H or C–O–C	532.7	37.8

chitosan is composed of both an amorphous and a crystalline component [23]. During chitosan degradation, the amorphous component was preferentially degraded, leaving the crystalline part intact. With further degradation, the amorphous layer peeled off and was dissolved in the reaction medium, and then the crystalline structure was destroyed, and the crystallinity decreased accordingly. Hence, the increase in the degree of crystallinity and the smoothing of the chitosan surface is likely the result of removal of the amorphous components on the surface of chitosan during the oxidative treatment by $H^•$, $^•OH$ and H_2O_2, which formed during the GDP treatment. Meanwhile, the increasing number of $–CH_2$ and $–CH_3$ groups in the GDP-modified chitosan is likely due to broken chitosan chains from the amorphous components. During the modification, the rough amorphous surface of chitosan was preferentially degraded and dissolved in the reaction medium.

3.2. Adsorption kinetics of dye on GDP-modified chitosan

For the practical application of chitosan in the treatment of dye pollutants, the kinetic behavior of the dye adsorption process was studied using chitosan particles modified using the GDP process at different currents and reaction times (Fig. 6). It is observed that C. I. Acid Red 73 uptake on GDP-modified chitosan was faster than adsorption on untreated chitosan. For the chitosan treated at 30 mA for 60 min and in 100 mA for 30 min, the amount of adsorption increased rapidly over the first 20 min, contributing to about 92.1% of the total adsorption. In contrast, dye adsorption on untreated chitosan was a much slower process that only removed 42.1% of the dye in 20 min.

This experiment also showed that the pretreatment time of chitosan influenced its adsorption behavior (Fig. 6a). When the modification time increased from 0 to 60 min, a 20% increase in adsorption efficiency was observed. As shown in Fig. 6b, the adsorption efficiency also increased with an increase in the GDP current used during modification. When the GDP current reached 100 mA, 98.4% of C. I. Acid Red 73 was removed within 60 min, and the adsorption efficiency was increased by ca. 20% compared with the untreated chitosan.

These results show that the GDP modification resulted in an improved adsorption of dye by chitosan over a shorter period of time. The applied current and the modification time are two crucial factors that lead to improvement in the removal efficiency of C. I. Acid Red 73 in water by GDP-modified chitosan. These improvements in dye adsorption may be due to the removal of the amorphous surface components; specific mechanisms will be discussed in detail below.

3.3. Adsorption isotherms of dye on GDP-modified chitosan

In order to further explore the difference of adsorption capacity between the untreated chitosan and GDP-modified chitosan, adsorption isotherms were measured at various initial dye concentrations in the presence of 2.0 g/L of the adsorbent at 25 °C. The Langmuir isotherm model, which is given below, was used to fit the experimental data [24]:

$$q_e = \frac{q_m b C_e}{1 + bC_e}$$

where q_e is the amount of dye adsorbed at equilibrium (mg/g), C_e is the equilibrium concentration of dye in the bulk solution (mg/L), b is the Langmuir constant related to energy (L/mg), and q_m is the adsorption capacity, defined as the maximum amount of dye forming a complete monolayer on the adsorbent surface (mg/g).

The experimental results were fitted to the linearized form of the Langmuir model below:

$$\frac{C_e}{q_e} = \frac{1}{bq_m} + \frac{1}{q_m} C_e$$

According to the literature [25], the essential features of the Langmuir isotherm can be expressed in terms of a separation factor or equilibrium parameter, R_L, that can be calculated from the following relationship:

$$R_L = \frac{1}{(1 + bC_0)}$$

where C_0 is the highest initial concentration (mg/L). The value of R_L indicates whether the isotherm is characteristic of irreversible adsorption ($R_L = 0$), favorable adsorption ($0 < R_L < 1$), unfavorable adsorption ($R_L > 1$), or linear adsorption ($R_L = 1$).

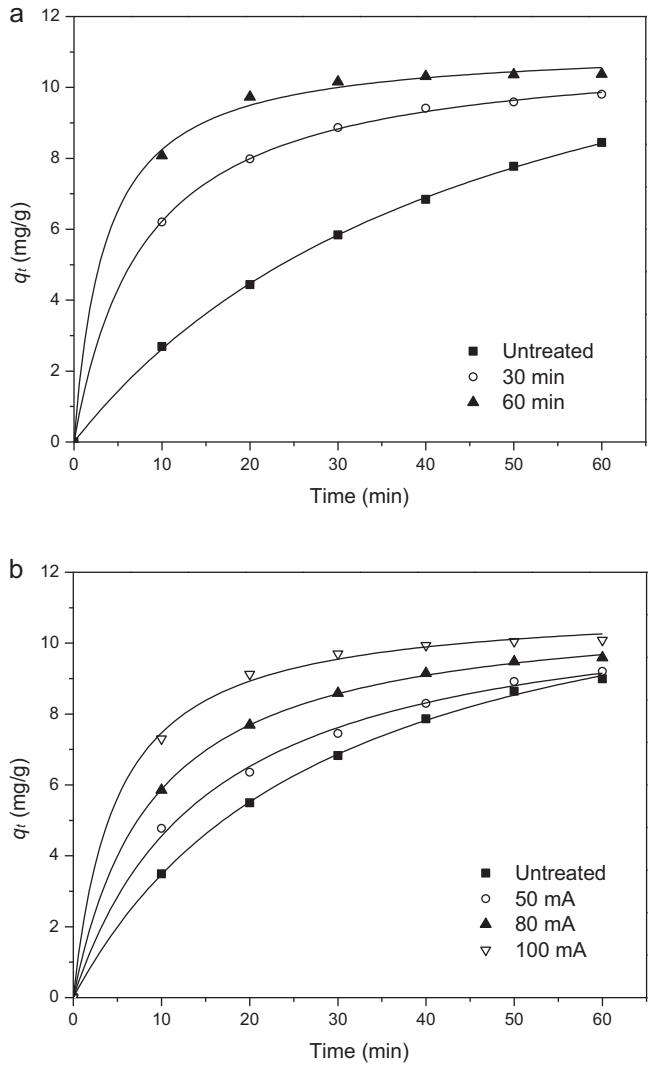

Fig. 6. Removal of C. I. Acid Red 73 (initial concentration 50 mg/L, 10 mL, pH = 6, room temperature) using untreated or modified chitosan (0.05 g). (a) Effect of the reaction time of the modification (GDP current: 80 mA; T = 25 °C); (b) effect of the GDP current on the modification (reaction time: 60 min; T = 25 °C).

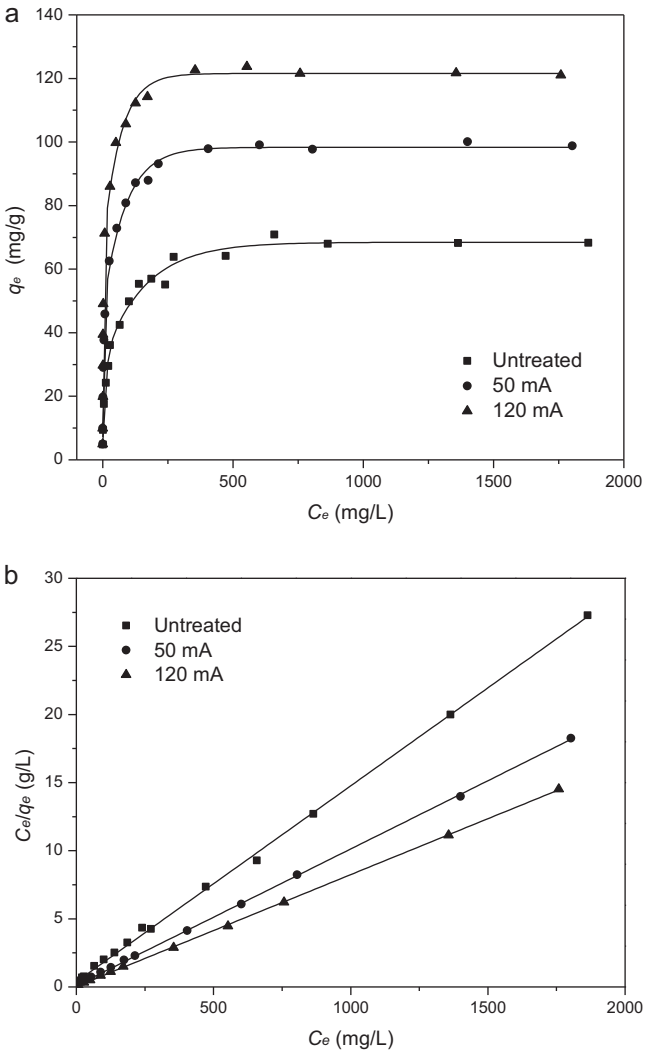

Fig. 7. Adsorption isotherm of C. I. Acid Red 73 on untreated and GDP-modified chitosan (modified under 50 and 120 mA at 25 °C for 60 min) at room temperature.

The results of the experimental data fitted to the Langmuir equation and the corresponding parameters are shown in Fig. 7 and Table 2. The values of the correlation coefficients (R^2) indicate that the sorption systems above closely follow the Langmuir model. From the model fitting, the maximum adsorption (q_m) and Langmuir constant (b) at different temperatures were determined from the slope and intercept of the Langmuir plots. The q_m values of AR 73 adsorption by chitosan followed the order of untreated chitosan < modified chitosan (GDP current: 50 mA) < modified chitosan (GDP current: 120 mA), implying that the chitosan modified by GDP had a higher maximum adsorption capacity in comparison with the untreated chitosan, and the higher the current used during the GDP modification, the higher the q_m values. All of the measured R_L values for both untreated and modified chitosan had values less than 1, indicating favorable adsorption.

Table 2
Langmuir parameters for the adsorption of C. I. Acid Red 73 by chitosan at room temperature.

Adsorbent	R^2	q_m (mg/g)	$b \times 10^{-3}$ (L/g)	R_L
Untreated chitosan	0.9989	69.54	0.0376	0.0131
Modified chitosan (50 mA)	0.9997	99.80	0.0926	0.0054
Modified chitosan (120 mA)	0.9999	121.80	0.2169	0.0023

3.4. Proposed mechanism

The mechanism most often cited for the adsorption of anionic dyes by chitosan in acidic solution is likely to be electrostatic interaction of the dye ions with protonated amino groups on the chitosan surface [26]. According to the literature, the H_2O_2-induced surface modification enhances the interaction between the dye and chitosan, owing to the increase of free hydroxyl and amine groups on the chitosan surface after the partial removal of amorphous components [19]. The hydrogen bonds linked between monomer units of different chains (intermolecular bonds) would affect the availability of amine groups in chitosan [27,28]. When the amorphous part of chitosan is preferentially degraded and removed, the hydrogen bonds between the amorphous and crystalline components are destroyed, resulting in an increase of free amine groups and –OH groups on the chitosan surface. Thus, the electrostatic interaction of the dye ions with the protonated amino groups on chitosan was enhanced, and the adsorption ability of chitosan was improved.

In the GDP modification system, the chemically active species $^{\bullet}OH$ and H_2O_2 play an important role in chitosan modification due to their strong oxidizing ability. At 530 V, GDP is created around a

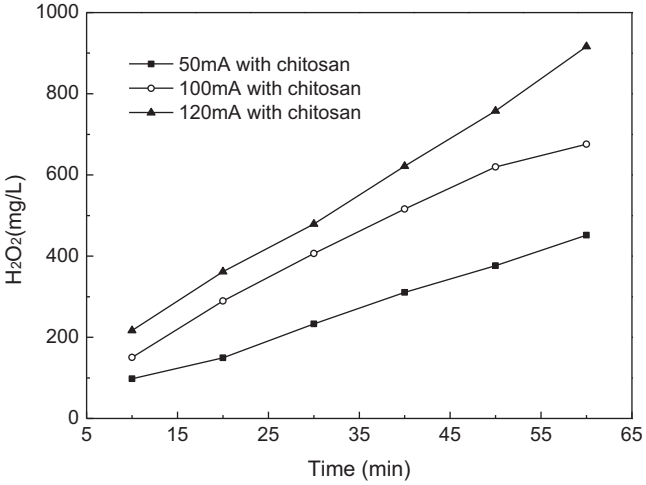

Fig. 8. Production of H_2O_2 at different currents during the glow discharge process.

pointed anode in the aqueous solution, causing formation of various chemically active species, such as H•, •OH and H_2O_2, due to bombardment of energetic H_2O^{+*} ions from the plasma.

$$H_2O^{+*} + nH_2O \rightarrow n^{\bullet}OH + nH^{\bullet} + H_2O^{+}$$

$$^{\bullet}OH + {}^{\bullet}OH \rightarrow H_2O_2$$

As shown in Fig. 8, the H_2O_2 gradually accumulated with increasing time under a certain discharge, and the concentration grew at elevated GDP currents. After discharge for 60 min at 120 mA, the concentration of H_2O_2 reached 900 mg/L. Importantly, this phenomenon agrees well with the results presented in Figs. 6 and 7, where the adsorption rate and adsorption capacity of chitosan were improved gradually with accumulation of H_2O_2 in the GDP modification system.

Additionally, to estimate the enhancement of electrostatic interactions, the zeta potential value of chitosan samples, which indicates the charge density at the chitosan surface, was also determined (Fig. 9). All chitosan dispersions possessed a positive zeta potential, and their values increased from 15.78 mV (untreated chitosan) to 26.76 mV and 24.60 mV with increasing modification time and GDP current, respectively. This result suggests that increasing dye adsorption after surface modification was possibly due to the increased electrostatic interaction between C. I. Acid Red 73 and chitosan. Meanwhile, the relative amount of $-NH_3^+$ on the chitosan surface (Table 1) indicates that almost no preliminary protonation of amine groups occurred on the chitosan surface during the pretreatment.

Overall, the proposed mechanism is presented as follows. During the oxidative degradation by active species, including H•, •OH and H_2O_2, which formed during the GDP treatment, the amorphous components on the chitosan surface were partially removed, resulting in an increase in the number of free amine and hydroxyl groups on the surface. This improved the adsorption of dyes due to the enhancement of electrostatic interactions between the dye and chitosan molecules.

3.5. Adsorption of other organic dyes

It is well known that the complicated structures of dye molecules, which vary with respect to their organic chains and the numbers and positions of functional groups, are directly related to their adsorption behavior. Thus, the same adsorption conditions used for C. I. Acid Red 73 were next applied to the removal of a variety of anionic dyes. Acid dyes, such as C. I. Acid Blue 25 (AB 25),

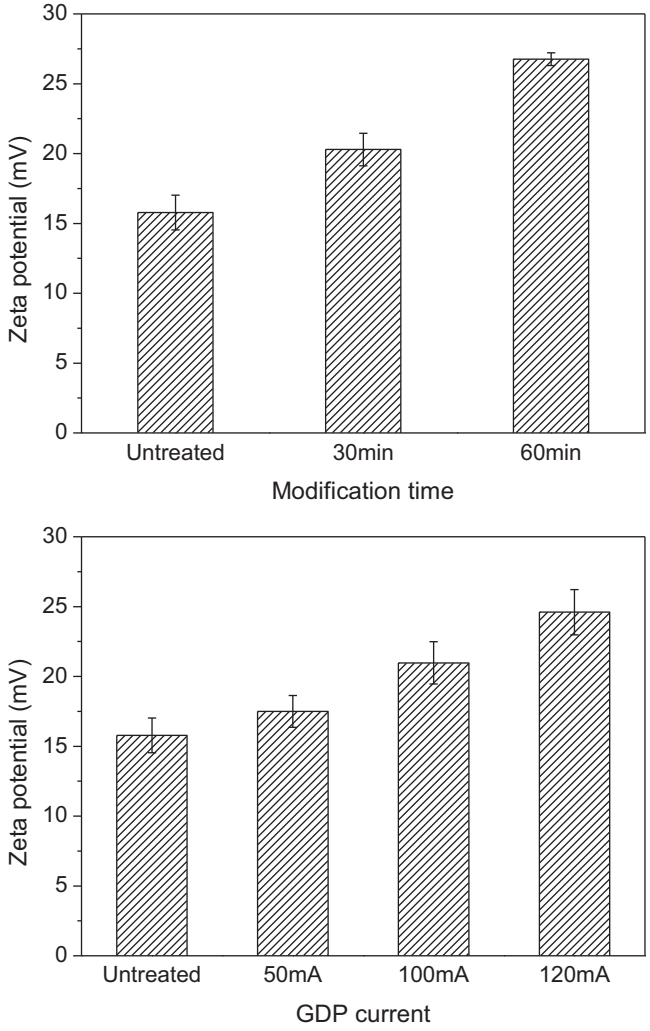

Fig. 9. Zeta potential of chitosan modified at different (a) reaction times (GDP current: 80 mA) and (b) GDP currents (reaction time: 60 min).

C. I. Acid Blue 40 (AB 40), C. I. Acid Blue 62 (AB 62), C. I. Acid Blue 113 (AB 113) and C. I. Acid Blue 193 (AB 193), and reactive dyes, such as C. I. Reactive Yellow 2 (RY 2), C. I. Reactive Yellow 18 (RY18), C. I. Reactive Red 11 (RR11), C. I. Reactive Red 24 (RR 24), C. I. Reactive

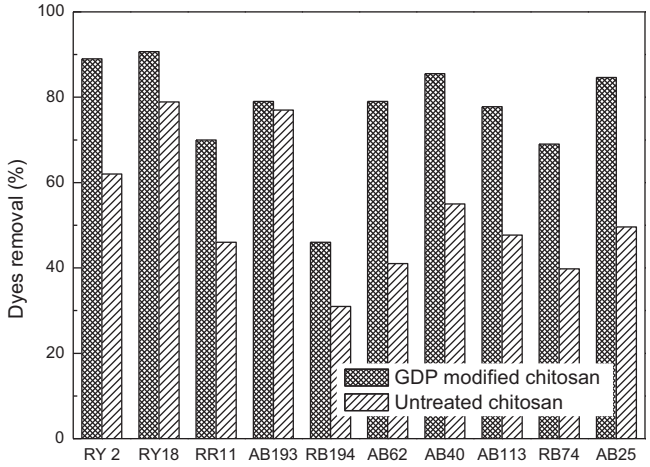

Fig. 10. Adsorption curves of other organic dyes (initial concentration: 50 mg/L, 10 mL, pH = 6, room temperature) on untreated (0.05 g) and modified chitosan (0.05 g; GDP current: 80 mA; reaction time: 60 min).

Blue 194 (RB 194) and C. I. Reactive Blue 74 (RB 74), were chosen as prototypical dye pollutants. The results are shown in Fig. 10, and the data suggest that GDP modification of chitosan improves the adsorption of both acid and reactive dyes to varying degrees.

4. Conclusions

In this study, glow discharge plasma in water is explored as a suitable and green approach to enhancing the adsorption properties of chitosan for dye removal. The results showed that the GDP treatment changed the morphology and crystallinity of chitosan particles, and that the number of $-CH_2$ and $-CH_3$ group in chitosan samples increased. Various pretreatment parameters, including discharge current and pretreatment time, played significant roles on the chitosan modification. C. I. Acid Red 73 uptake on GDP-modified chitosan was faster than adsorption on untreated chitosan. The value of maximum adsorption for AR 73 by chitosan followed the order of untreated chitosan < modified chitosan (GDP current: 50 mA) < modified chitosan (GDP current: 120 mA), implying that the chitosan modified by GDP had a higher maximum adsorption capacity than the untreated chitosan. Thus, we conclude that this technically facile, highly efficient and cost effective glow discharge plasma is an attractive pretreatment method for environmental adsorption materials.

Acknowledgments

This study was supported by the Qianjiang Talent Scheme, Zhejiang Province, China (No. 2011R10045), the National Basic Research Program of China (No. 2009CB421603) and the Fundamental Research Funds for the Central Universities.

References

[1] G. Crini, Non-conventional low-cost adsorbents for dye removal: a review, Bioresour. Technol. 97 (2006) 1061–1085.
[2] Y.Z. Wen, W.Q. Liu, Z.H. Fang, W.P. Liu, Effects of adsorption interferents on removal of Reactive Red 195 dye in wastewater by chitosan, J. Environ. Sci. China 17 (2005) 766–769.
[3] M. Thanou, M.T. Nihot, M. Jansen, J.C. Verhoef, H.E. Junginger, Mono-*N*-carboxymethyl chitosan (MCC), a polyampholytic chitosan derivative, enhances the intestinal absorption of low molecular weight heparin across intestinal epithelia *in vitro* and *in vivo*, J. Pharm. Sci. 90 (2001) 38–46.
[4] M.S. Chiou, H.Y. Li, Adsorption behavior of reactive dye in aqueous solution on chemical cross-linked chitosan beads, Chemosphere 50 (2003) 1095–1105.
[5] M.X. Li, S.L. Cheng, H.S. Yan, Preparation of crosslinked chitosan/poly(vinyl alcohol) blend beads with high mechanical strength, Green Chem. 9 (2007) 894–898.
[6] K.Z. Elwakeel, Removal of Reactive Black 5 from aqueous solutions using magnetic chitosan resins, J. Hazard. Mater. 167 (2009) 383–392.
[7] M.A. Malik, A. Ghaffar, S.A. Malik, Water purification by electrical discharges, Plasma Sources Sci. Technol. 10 (2001) 82–91.
[8] Y.Z. Wen, X.Z. Jiang, W.P. Liu, Degradation of 4-chlorophenol by high-voltage pulse discharges combine with ozone, Plasma Chem. Plasma Process. 22 (2002) 175–185.
[9] X.L. Yin, W.J. Bian, J.W. Shi, 4-Chlorophenol degradation by pulsed high voltage discharge coupling internal electrolysis, J. Hazard. Mater. 166 (2009) 1474–1479.
[10] Y.H. Bai, J.R. Chen, Y. Yang, L.M. Guo, C.H. Zhang, Degradation of organophosphorus pesticide induced by oxygen plasma: effects of operating parameters and reaction mechanisms, Chemosphere 81 (2010) 408–414.
[11] Y.J. Liu, X.Z. Jiang, Phenol degradation by a nonpulsed diaphragm glow discharge in an aqueous solution, Environ. Sci. Technol. 39 (2005) 8512–8517.
[12] J.Z. Gao, D.P. Ma, X. Guo, A.X. Wang, Y. Fu, J.L. Wu, W. Yang, Degradation of anionic dye eosin by glow discharge electrolysis plasma, Plasma Sci. Technol. 10 (2008) 422–427.
[13] Y. Wen, X. Jiang, Degradation of acetophenone in water by pulsed corona discharge, Plasma Chem. Plasma Process. 20 (2000) 343–351.
[14] Y.Z. Wen, X.Z. Jiang, Pulsed corona discharge-induced reactions of acetophenone in water, Plasma Chem. Plasma Process. 21 (2001) 345–354.
[15] Y.Z. Wen, X.Z. Jiang, W.P. Liu, Degradation of 4-chlorophenol by high-voltage pulse corona discharges combined with ozone, Plasma Chem. Plasma Process. 22 (2002) 175–185.
[16] G.L. Chen, S.H. Chen, W.R. Feng, W.X. Chen, S.Z. Yang, Surface modification of the nanoparticles by an atmospheric room-temperature plasma fluidized bed, Appl. Surf. Sci. 254 (2008) 3915–3920.
[17] R. Morent, N. De Geyter, T. Desmet, P. Dubruel, C. Leys, Plasma surface modification of biodegradable polymers: a review, Plasma Process. Polym. 8 (2011) 171–190.
[18] T. Desmet, R. Morent, N. De Geyter, C. Leys, E. Schacht, P. Dubruel, Nonthermal plasma technology as a versatile strategy for polymeric biomaterials surface modification: a review, Biomacromolecules 10 (2009) 2351–2378.
[19] C.S. Shen, Y.Z. Wen, X.D. Kang, W.P. Liu, H_2O_2-induced surface modification: a facile, effective and environmentally friendly pretreatment of chitosan for dyes removal, Chem. Eng. J. 166 (2011) 474–482.
[20] G.E. Eisenberg, Colorimetric determination of hydrogen peroxide, Ind. Eng. Chem. 15 (1943) 327–328.
[21] N. Sakkayawong, P. Thiravetyan, W. Nakbanpote, Adsorption mechanism of synthetic reactive dye wastewater by chitosan, J. Colloid Interface Sci. 286 (2005) 36–42.
[22] W. Yue, P.J. Yao, Y.N. Wei, Influence of ultraviolet-irradiated oxygen on depolymerization of chitosan, Polym. Degrad. Stab. 94 (2009) 851–858.
[23] F. Tian, Y. Liu, K. Hu, B.Y. Zhao, Study of the depolymerization behavior of chitosan by hydrogen peroxide, Carbohydr. Polym. 57 (2004) 31–37.
[24] S. Chatterjee, M.W. Lee, S.H. Woo, Adsorption of congo red by chitosan hydrogel beads impregnated with carbon nanotubes, Bioresour. Technol. 101 (2010) 1800–1806.
[25] M.F. Sawalha, J.R. Peralta-Videa, J. Romero-González, J.L. Gardea-Torresdey, Biosorption of Cd(II), Cr(III), and Cr(VI) by saltbush (Atriplex canescens) biomass: thermodynamic and isotherm studies, J. Colloid Interface Sci. 300 (2006) 100–104.
[26] G. Crini, P.M. Badot, Application of chitosan, a natural aminopolysaccharide, for dye removal from aqueous solutions by adsorption processes using batch studies: a review of recent literature, Prog. Polym. Sci. 33 (2008) 399–447.
[27] E. Guibal, E. Touraud, J. Roussy, Chitosan interactions with metal ions and dyes: dissolved-state vs. solid-state application, World J. Microbiol. Biotechnol. 21 (2005) 913–920.
[28] M. Rinaudo, Chitin and chitosan: properties and applications, Prog. Polym. Sci. 31 (2006) 603–632.